Comparative Study the Impact of Single and Double Vacancy Defects in BC3 Nanosheet on the Acetaminophen Detection

Saeideh Ebrahimiasl (saeidehebrahimiasl@gmail.com)
Islamic Azad University
Akram Hosseinian
University of Tehran

Research Article

Keywords: Vacancy defect, Work function, Electrical bang gap, Magnetic properties

Posted Date: February 9th, 2021

DOI: https://doi.org/10.21203/rs.3.rs-179104/v1

Comparative study the impact of single and double vacancy defects in BC_3 nanosheet on the acetaminophen detection

Saeideh Ebrahimiasl[a*] and Akram Hosseinian[b]

[a]Department of Chemistry, Ahar Branch, Islamic Azad University, Ahar, Iran

[b]Department of Engineering Science, College of Engineering, University of Tehran, P.O. Box 11365-4563, Tehran, Iran

Email address: saeidehebrahimiasl@gmail.com

Abstract

Density functional theory (DFT) calculations was used to investigate the interaction between the prefect and defected boron carbide (BC_3) monolayer nanosheet and conventional acetaminophen (AP) drug. The obtained findings indicate no considerable interaction between BC_3 nanosheet and AP drug. Thus, perfect BC_3 is not highly sensitive against AP presence regarding weak interactions. We explored if introducing single vacancy (SV) and double vacancy (DV) defect in prefect BC_3 nanosheet can enhance the interaction with AP drug. The adsorption energy of AP drug on the DV-BC_3 and SV- BC_3 surface were calculated about -15.32 and -23.78 kcal/mol, respectively. After AP adsorption, a considerable change of bang gap and work function of DV-BC_3 and SV-BC_3 was observed while only the electrical bang gap of perfect BC_3 was changed after AP adsorption and the work function change was negligible. It can be concluded that both defected BC_3 sheets can act as both electrical and work function sensor types while the perfect BC_3 can only act as an electrical sensor. The adsorption energy is remarkably changed in media with higher dielectric constant. Additionally, AP adsorption dramatically changes the magnetic properties of DV-BC_3.

Keywords: Vacancy defect, Work function, Electrical bang gap, and Magnetic properties

1. Introduction

Social development criteria such as education, lifestyle, and better medicines have promoted the human health standards during last 50 years [1]. However, there has been an increase in the usage of pharmaceuticals for lengthening life and also to treat a variety of diseases [2]. Acetaminophen (AP) (N-acetyl-P-aminophenol) is a conventional painkillers drug has been widely used to diminish fever and pain [3]. The AP disposal in waste water and ground water has been an environmental concern during last decades [4]. According to analytical chemistry literature, the detection concentration range of AP is about 100-1000 to ng^{-1} which challenges it an emerging waste water treatment concern worldwide [5-11]. Additionally, increasing AP value in drinking water has resulted in serious diseases including heart, gastro-intestine, and kidney disorders[12, 13]. Furthermore, the AP overdose may lead to health hepato- and nephro-toxic [14, 15]. AP detection in water and waste water is of a great deal of importance regarding the mentioned health concerning challenges and a straightforward and simple method of ACE detection is critical. conventional analytical methods of AP detection pharmaceutical and biological media include spectrophotometry [16], high performance liquid chromatography (HPLC) [17], gas chromatography (GC) [18], titrametry [19], and chemiluminescence [20]. An efficient and appropriate extraction process is a requisite of all above mentioned methods before detection procedure. Although mentioned detection techniques often meet the standard requirements in miscellaneous samples, the intricate procedure and high costs may limit their widespread application. Nanomaterials are the most promising candidates for the detection of chemical species owing to their specificities such as high stability, considerably high specific surface area and high biocompatibility [21-23]. According to literature, many studies have been conducted based on their specific adjustable features and their exclusive application [24]. Nanomaterial-based detectors

have been widely investigated regarding their high sensitivity, low response time, low cost and capability of direct detection of AP in real-time.

The promising candidate to play effective role in energy storage, sensing, composites are carbon based nanomaterial. In addition to one component carbon based sheets, multicomponent structures of these sheets have been widely reported mainly including boron and nitrogen atoms [25, 26]. These BCN monolayers, with elemental stoichiometries such as BN, BC_2N, and BC_3, show noticeable electronic specificities which can be applied for specific uses [27]. Both experimental (arch-discharge) and first principle methods have been applied to confirm the stability and existence of BC_3 nanomaterial [28-30]. There are convincing experimental and theoretical evidences that verify the stability and existence of BC_3 nanodomains in nanotube and sheet structure upon the replacement of boron atom in CNTs [31, 32]. Strictly speaking, similar justifications have been reported to discuss the stability of both BC_3 sheet. Several theoretical approaches have been proposed to study the structural and electronic identity of BC_3 sheet [33-35]. Almost all types of BC_3 sheets and also nanotube counterparts such as (n, 0) zigzag and (n, n) armchair, are classified as small-gap semiconductors [36]. Like other nanosheet, some imperfections may be introduced either during the synthesis or because of applied stress in experimentally available BC_3 nanosheet [37, 38]. Most frequently reported defects include antisites, vacancies, and topological defects. These defects often result in electronic, mechanical, and optical properties of nanotubes. Additionally, an interesting type of defect, obtained by rotation of a chemical bond by 90°, is called Stone-Wales (SW) topological defects mainly reported in CNTs and boron nitride nanotubes (BNNTs) [39-45].

In the present study, the adsorption behavior of AP drug on both perfect and defected BC_3 nanosheet substrates toward AP adsorbate was investigated through density functional theory

(DFT) calculations. Considering the feasibility of mentioned sheets to act as sensors is targeted as well. The effect of dielectric constant, as the main factor determining the solvent specificities, on tendency of AP adsorbate toward BC_3 sheet. Finally, the mechanistic study of adsorption process was done by applied NICS calculations.

2. Computational details

Quantum chemical calculations were done through density functional theory (DFT) by GAMESS program package [46]. All studied nanotube structures were geometrically optimized at the level of M06-2X/6-31G (d) [47]. Also, the aromaticity of the nanotubes was analyzed in GIAO- M06-2X/6-31G (d) level by nucleus independent chemical shift (NICS) value at the center of molecule as well as the nanotube axes to investigate the shielding effect of the whole tube. The adsorption energy (E_{ad}) upon complexation between the BC_3 nanosheet and AP drug is defined as:

$$E_{ad}=E_{sheet\text{-}AP}-E_{sheet}-E_{AP}+\delta_{BSSE} \quad (1)$$

In which E_{sheet} and E_{AP} are the total energy of BC_3 nanosheet and AP drug, respectively. $E_{sheet\text{-}AP}$ is also, the total energy of the BC_3-AP complex. We used counterpoise method to predict δ (BSSE, basis set superposition error).

3. Results and discussion

3.1.Adsorption of AP drug on the perfect BC_3 nanosheet

The interaction of AP drug with perfect BC_3 surface was investigated to study the adsorption behavior of adsorbent. The adsorption behavior of BC_3 toward AP species can elucidate whether this nanotube can effectively adsorb and detect this AP drug. Similar to main 2D grapheme and BN sheets, BC_3 sheet has a hexagonal lattice. As can be seen in **Fig.1**, BC_3 unit cell consists of six

C atoms and two B atoms. According to optimized geometry data, the B–C bond and C–C bond lengths are 1.56 and 1.42 Å, respectively. Also, the band gap of the BC_3 monolayer is obtained about 2.33 eV as shown in **Fig. 1**, which is in agreement with the reported bond distance values reported at literature [36]. Considering the adsorption of AP drug onto BC_3 substrate, the most feasible interaction configuration is considered of O atoms of adsorbates close to the boron atom of BC_3. The BC_3-AP complex is schematically shown in **Fig. 2**. Having fully optimized the structure of BC_3-AP complex, the adsorption energy was extracted by considering the BSSE correction. According to ab initio calculation findings, it can be concluded that the AP drug are not strongly interacted to the BC_3 surface by releasing the low energy of around -3 to -5 kcal/mol which indicates that this kind of adsorption can be classified as physisorption. The calculated adsorption energy values for both configurations under evaluation is summarized in Table 1. Remarkably negative adsorption energy values were obtained for almost all complexes and hence BC_3 sheet is stabilized after AP adsorption. Charge transfer analysis were carried out between interacting entities to consider the interaction nature of involved species. Negligible 0.053 e charges transfer between AP and BC_3 was reported according to Hirshfeld charge analysis. Very low charge transfer values corresponds to a low adsorption energy AP on BC_3 as listed in table 1.

3.2.Adsorption of AP drug on the defected BC_3 nanosheet

As mentioned before, the interaction and adsorption of perfect BC_3 nanosheet is not strong enough to capture AP effectively which is strictly needed for sensing and monitoring of AP drug. Therefore, the tendency of BC_3 substrate toward AP adsorbent and consequently the adsorption ability should be promoted. For this purpose, the effect of structural defects on the enhancement of potential adsorption of adsorbent was investigated. Experimentally, different detects have been applied in this type of materials such as: Stone-Waals and single and double vacancy and etc. [44].

Vacancy defects have been widely studied as point defect types and their effects have on physicochemical nature of nanomaterials have been examined [40]. when an atom is missing from a lattice sites, the defect is known as a "vacancy" also known as a Schottky [40]. The single vacancy (SV) and double vacancy (DV) are the importance defect in which an atom is missing from its regular atomic site. It can be noted that vacancies are often created within solidification as a result of the vibration and local rearrangement of atoms [40].

As shown in **Fig.3**, the optimized SV and DV defect structure of BC_3. The electronic properties of SV and DV of BC_3 significantly changed compared to the perfect one. The band gap value of SV and DV of BC_3 were calculated about 1.86 and 1.74 eV, respectively. Having attached the AP drug to defected site of modeled BC_3 surface, full optimization was done the same level of theory. After optimizing the structures of the complex, the adsorption energy was determined and the data are summarized in Table 1. The optimized of AP drug on the SV-BC_3 and SV-BC_3 surface as shown in **Fig.4**. A significant enhancement of adsorption energy, -15.32 and -23.78 kcal/mol, were observed for AP on the SV-BC_3 and SV-BC_3 surface, respectively. According to obtained data, it can be noted that the adsorption of AP on DV-BC_3 are stronger than the SV-BC_3 and perfect BC_3. It was clearly found that the adsorbed molecule was attached closer to the DV-BC_3 surface compared to SV-BC_3 and perfect BC_3.

Total charge density changes were monitored to investigate the interaction process. **Fig. 5(a-b)** shows the calculated total charge density of most stable structure for AP species on both DV-BC_3 and perfect BC_3 sheets. The picture shows that there is charge accommodation between the interaction region of AP molecule and DV-BC_3. Contrarily, no evidence is found in AP drug and perfect BC_3 system for the charge population in the interacting region. Thus, a strength interaction between AP and DV-BC_3 and weak interaction between AP drug and perfect BC_3 are eligible based

on adsorption studies. Also, Hirshfeld approach considering the charge population variations demonstrates a significant charge transfer of AP adsorbent and DV-BC_3 substrate with about half charge (0.597 e) while a very smaller charge transfer was observed, 0.053 e, between AP and perfect BC_3.

3.3.Evolution the electric response of DV-BC_3 and SV-BC_3 to AP drug

Considerable electronic changes, resulted from both orbital mixing and the charge transfer of the DV-BC_3 and SV-BC_3 sheet, are significant criteria for sensing applications. The electrical conductivity (σ) of materials is related to the conventional exponential band gap equation as follow:

$$\sigma \propto \exp(-E_g/2KT) \quad (2)$$

Here, k_B and T are the Boltzmann constant and absolute temperature, respectively. Apparently, a small change in the energy bond gap considerably shifts the electrical conductivity. The energy bond gap of DV-BC_3 (1.84 eV) and SV-BC_3 (1.76 eV) decreases to 1.16 and 0.94 eV upon interaction with AP drug, respectively. Also, can be calculated the reopens of sensor by using band gap changes as follows equation:

$$R = \frac{\sigma}{\sigma_0} \quad (3)$$

which σ and σ_0 are the electrical conductivity signals of the DV-BC_3 after and before of AP drug, respectively. From Eq. (3), one can write:

$$R = \exp\left[-(E_g - E_{g1}) / 2kT\right] = \exp(-\Delta E_g / kT) \quad (4)$$

Using Eq. (4), the response of the DV-BC_3 and SV-BC_3 were predicted to be 54323 and 80291, respectively and indicating sensitivity of the DV-BC_3 to AP because of a high response value. It should be noted that absolute value of ΔE_g is used for calculation of sensing responses. Therefore, it can be a promising electronic sensor for monitoring of AP drug.

3.4.NICS investigation

In compounds with π-electron systems with an applied external magnetic field, The induced ring current results in generation of an induced magnetic field in the opposite direction of the exerted magnetic field at the aromatic ring center [48]. Regarding the fact that the aromaticity cannot be observed by many examinations, acquiring any data about it should be provided from magnetic specificities [48]. Among most known magnetic methods to study the aromaticity, Nuclear magnetic resonance (NMR) chemical shifts and diamagnetic susceptibilities are the most conventional and straightforward ones. Diatropic compounds are defined as aromatic chemicals with noticeably high diamagnetic susceptibility while paratropic compounds are antiaromatic. In magnetic study of carbon nanotubes, the observed magnetic field inside the tube is resulted from diamagnetism and can be attributed to the ring currents in the molecular orbitals. Among all conventional magnetic parameters, the nucleus independent chemical shift (NICS) has been reported as a straightforward and applicable probe to consider the aromaticity of most compounds. The characterization of aromaticity of molecules by NICS has been validated by many studies. Compared to 3He-NMR chemical shift as a validated tool to study nanotubes, the same values are obtained from computational NICS at the molecule center. It's noteworthy that negative and positive NICS values denote the aromatic and antiaromatic specificities, respectively. The calculated NICS values of DV-BC_3 before and after adsorption of AP species at the sheet center as well as the Z-axis of BC_3. Negative NICS values were obtained for all investigated compounds

indicating that all of them demonstrate aromatic nature. The NICS factors were obtained about -29.33 and 12.84 ppm for DV-BC_3@AP and DV-BC_3, respectively. DV-BC_3@AP complex has the highest negative NICS value compared to the rest of the systems which indicates that DV-BC_3 is able to detect AP at the presence of a magnetic field of specific intensity. It can be concluded that the lone pair O atom electrons of AP molecule modify the uniformity in ring current and the π-resonance system, exhibiting an ordered π-resonance in the parent DV-BC_3, increases. The aromaticity was increased and negative NICS value was obtained during the adsorption process of AP drug.

3.5.Effect of solvents dielectric on the adsorption behavior of AP drug

The chemical stability and adsorption behavior of AP drug have been studied in the presence of different solvents regarding their dielectric constant as a criterion of solvent polarity. According to findings, the solubility of this AP drug s mainly affected by increasing of solvent polarity. The solvation energy can be calculated by using equation: $\Delta E_{solv} = E_{solv} - E_{gas}$. Comparison between E_{ad} calculated in both gas and solution phases showed that interactions are stronger in solution phase and more negative E_{ad} values were obtained. For example, the E_{ad} of AP in gas phase is −23.78 kcal/mol that increase to −51.96 kcal/mol in water. In the solvent with the small dielectric constant compared to water (acetonitrile, ε = 38.8), the E_{ad} is −39.77 kcal/mol that is increased the E_{ad} about 65.22% in comparison to gas phase. **Fig. 6** shows the value of E_{ad} in the many of solvent with various dielectric constant (ε).

As can be seen, the value of E_{ad} was decreasing significantly by decreasing the dielectric constant solvent. As mentioned above, E_{ad} increases with the increasing dielectric constant. The solubility of AP increases as the dielectric constant is increased which is attributed to the solvent cage effect.

In other words, by increasing solvent polarity, the solubility of AP molecules has increased and the value of adsorption energy has consequently increased.

3.6. Work function

The work function variation of defect and perfect BC_3 were investigated for further evaluation of AP sensing. According to empirical investigations, the mechanism of the Φ-type gas sensors is defined based on the Kelvin process in which a Kelvin oscillator device is applied to evaluate Φ of the sample before and after the adsorption of AP on BC_3. If AP drug adsorption substantially alters the Φ of the adsorbent, it can shift the gate voltage resulting in producing an electrical noise that facilitates the AP detection eventually [49]. In sensor-related studies, the minimum energy required to extract one electron from the Fermi level of a material to an infinite distance is often represented as Φ:

$$\Phi = V_{el(+\infty)} - E_F \quad (5)$$

Eq.5 defines the electron electrostatic potential energy as V_{el} (+∞) which is relatively far from the material surface and is presumed to be negative, and EF is Fermi level energy. By Assuming V_{el} (+∞) = 0, according to the Eq. 5, Φ = -EF, the Fermi level energy is estimated as:

$$E_F = E_{HOMO} + (E_{LUMO} - E_{HOMO})/2 \quad (6)$$

Having considered the Richardson Dushman relation (Eq.7), there is a relationship between the Φ value and the current densities of the electron, hence the Fermi level varies as a function of Φ variation, which is related to the the field emission change [50]:

$$j = AT^2 \exp(-\Phi/kT) \quad (7)$$

here A is the constant of Richardson (A/m^2), and T is the absolute temperature (K). Correspondingly, the electron current density released from the BC_3 surface has a significantly change and the nanosheet can be regarded as an AP adsorption Φ-type sensor. The work function of AP drug adsorbed on the DV-BC_3, SV-BC_3 and BC_3 decreases to 4.49 to 3.54 eV, 4.81 to 3.65 eV and 5.32 to 4.94 eV, respectively. The reduction of DV-BC_3 and SV-BC_3 work function after AP drug adsorption is about 33.50% higher compared to perfect BC_3. As a result, the DV-BC_3 and SV-BC_3 are both electrical and work function sensor for AP detection, while the perfect BC_3 is only electrical sensor.

3.7.Recovery time

The recovery time of a sensing material is often considered as an important factor to evaluate the applicability of a gas sensor and is defined according to a conventional transition state theory as follows [51]:

$$\tau = \upsilon^{-1}\exp(E_{ad}/kT) \quad (8)$$

Here, υ^{-1} is the attempt frequency. According on this equation, a considerably increased (more negative) energy corresponds to a much longer recovery time. The recovery time of AP drug on DV-BC_3 was measured about 769 *ms.* This low recovery time value shows a short recovery time of AP drug from DV-BC_3 surface.

4. Conclusion

DFT calculations were applied to study the tendency of both perfect and defected BC_3 nanosheet toward the interaction of AP drug in gas and solvent media. The main conclusions are as follows:

i) Both vacancy defect in BC_3 sheet were improved the interaction with AP drug based on the adsorption energy value.

ii) The DV-BC_3 and SV-BC_3 sheet can act are both electrical and work function type sensors, while the perfect BC_3 is the only an electrical sensor.

iii) It can be used the magnetic properties as an in another parameter for sensing of AP drug on the DV-BC_3 sheet.

iv) The value of E_{ad} was decreased significantly by decreasing the dielectric constant solvent.

Disclosure statement:

Conflicts of Interest: None

Funding: None

Ethical Approval: Not required

References

[1] Lichtenberg, F.R. The impact of new drug launches on longevity: evidence from longitudinal, disease-level data from 52 countries, 1982–2001. International journal of health care finance and economics. 2005, 5, 47-73.

[2] Lu, Y., Hernandez, P., Abegunde, D., Edejer, T. The world medicines situation 2011. Geneva: Medicine expenditures World Health Organization. 2011, 35-8.

[3] Adhikari, B.-R., Govindhan, M., Chen, A. Sensitive detection of acetaminophen with graphene-based electrochemical sensor. Electrochimica Acta. 2015, 162, 198-204.

[4] Blair, B.D., Crago, J.P., Hedman, C.J., Klaper, R.D. Pharmaceuticals and personal care products found in the Great Lakes above concentrations of environmental concern. Chemosphere. 2013, 93, 2116-23.

[5] Bound, J.P., Voulvoulis, N. Predicted and measured concentrations for selected pharmaceuticals in UK rivers: implications for risk assessment. Water Research. 2006, 40, 2885-92.

[6] Petrie, B., Barden, R., Kasprzyk-Hordern, B. A review on emerging contaminants in wastewaters and the environment: current knowledge, understudied areas and recommendations for future monitoring. Water research. 2015, 72, 3-27.

[7] Gros, M., Petrović, M., Ginebreda, A., Barceló, D. Removal of pharmaceuticals during wastewater treatment and environmental risk assessment using hazard indexes. Environment international. 2010, 36, 15-26.

[8] Radjenovic, J., Petrovic, M., Barceló, D. Analysis of pharmaceuticals in wastewater and removal using a membrane bioreactor. Analytical and bioanalytical chemistry. 2007, 387, 1365-77.

[9] Pascual-Aguilar, J., Andreu, V., Picó, Y. An environmental forensic procedure to analyse anthropogenic pressures of urban origin on surface water of protected coastal agro-environmental wetlands (L'Albufera de Valencia Natural Park, Spain). Journal of hazardous materials. 2013, 263, 214-23.

[10] Guerra, P., Kim, M., Shah, A., Alaee, M., Smyth, S. Occurrence and fate of antibiotic, analgesic/anti-inflammatory, and antifungal compounds in five wastewater treatment processes. Science of the Total Environment. 2014, 473, 235-43.

[11] Sites, B.D., Beach, M.L., Davis, M.A. Increases in the use of prescription opioid analgesics and the lack of improvement in disability metrics among users. Regional Anesthesia & Pain Medicine. 2014, 39, 6-12.

[12] Clark, R., Fisher, J.E., Sketris, I.S., Johnston, G.M. Population prevalence of high dose paracetamol in dispensed paracetamol/opioid prescription combinations: an observational study. BMC clinical pharmacology. 2012, 12, 11.

[13] Doherty, M., Hawkey, C., Goulder, M., Gibb, I., Hill, N., Aspley, S., et al. A randomised controlled trial of ibuprofen, paracetamol or a combination tablet of ibuprofen/paracetamol in community-derived people with knee pain. Annals of the rheumatic diseases. 2011, 70, 1534-41.

[14] Roberts, E., Nunes, V.D., Buckner, S., Latchem, S., Constanti, M., Miller, P., et al. Paracetamol: not as safe as we thought? A systematic literature review of observational studies. Annals of the rheumatic diseases. 2016, 75, 552-9.

[15] Mazaleuskaya, L.L., Sangkuhl, K., Thorn, C.F., FitzGerald, G.A., Altman, R.B., Klein, T.E. PharmGKB summary: pathways of acetaminophen metabolism at the therapeutic versus toxic doses. Pharmacogenetics and genomics. 2015, 25, 416.

[16] Săndulescu, R., Mirel, S., Oprean, R. The development of spectrophotometric and electroanalytical methods for ascorbic acid and acetaminophen and their applications in the analysis of effervescent dosage forms. Journal of pharmaceutical and biomedical analysis. 2000, 23, 77-87.

[17] Ravisankar, S., Vasudevan, M., Gandhimathi, M., Suresh, B. Reversed-phase HPLC method for the estimation of acetaminophen, ibuprofen and chlorzoxazone in formulations. Talanta. 1998, 46, 1577-81.

[18] Trettin, A., Zoerner, A.A., Böhmer, A., Gutzki, F.-M., Stichtenoth, D.O., Jordan, J., et al. Quantification of acetaminophen (paracetamol) in human plasma and urine by stable isotope-dilution GC–MS and GC–MS/MS as pentafluorobenzyl ether derivative. Journal of Chromatography B. 2011, 879, 2274-80.

[19] Burgot, G., Auffret, F., Burgot, J.-L. Determination of acetaminophen by thermometric titrimetry. Analytica chimica acta. 1997, 343, 125-8.

[20] Ruengsitagoon, W., Liawruangrath, S., Townshend, A. Flow injection chemiluminescence determination of paracetamol. Talanta. 2006, 69, 976-83.

[21] Hibino, H., Kageshima, H., Kotsugi, M., Maeda, F., Guo, F.-Z., Watanabe, Y. Dependence of electronic properties of epitaxial few-layer graphene on the number of layers investigated by photoelectron emission microscopy. Physical Review B. 2009, 79, 125437.

[22] Lee, C., Yan, H., Brus, L.E., Heinz, T.F., Hone, J., Ryu, S. Anomalous lattice vibrations of single-and few-layer MoS2. ACS nano. 2010, 4, 2695-700.

[23] Hoshino, A., Fujioka, K., Oku, T., Suga, M., Sasaki, Y.F., Ohta, T., et al. Physicochemical properties and cellular toxicity of nanocrystal quantum dots depend on their surface modification. Nano Letters. 2004, 4, 2163-9.

[24] Hubbell, J.A., Chilkoti, A. Nanomaterials for drug delivery. Science. 2012, 337, 303-5.

[25] Kouvetakis, J., Sasaki, T., Shen, C., Hagiwara, R., Lerner, M., Krishnan, K., et al. Novel aspects of graphite intercalation by fluorine and fluorides and new B/C, C/N and B/C/N materials based on the graphite network. Synthetic metals. 1989, 34, 1-7.

[26] Yao, B., Chen, W., Liu, L., Ding, B., Su, W. Amorphous B–C–N semiconductor. Journal of applied physics. 1998, 84, 1412-5.

[27] Azevedo, S., De Paiva, R. Structural stability and electronic properties of carbon-boron nitride compounds. EPL (Europhysics Letters). 2006, 75, 126.

[28] Weng-Sieh, Z., Cherrey, K., Chopra, N.G., Blase, X., Miyamoto, Y., Rubio, A., et al. Synthesis of B x C y N z nanotubules. Physical Review B. 1995, 51, 11229.

[29] Miyamoto, Y., Cohen, M.L., Louie, S.G. Theoretical investigation of graphitic carbon nitride and possible tubule forms. Solid state communications. 1997, 102, 605-8.

[30] Miyamoto, Y., Rubio, A., Louie, S.G., Cohen, M.L. Electronic properties of tubule forms of hexagonal BC 3. Physical Review B. 1994, 50, 18360.

[31] Carroll, D., Redlich, P., Blase, X., Charlier, J.-C., Curran, S., Ajayan, P., et al. Effects of nanodomain formation on the electronic structure of doped carbon nanotubes. Physical Review Letters. 1998, 81, 2332.

[32] Fuentes, G., Borowiak-Palen, E., Knupfer, M., Pichler, T., Fink, J., Wirtz, L., et al. Formation and electronic properties of BC 3 single-wall nanotubes upon boron substitution of carbon nanotubes. Physical Review B. 2004, 69, 245403.

[33] Hernandez, E., Goze, C., Bernier, P., Rubio, A. Elastic properties of C and B x C y N z composite nanotubes. Physical Review Letters. 1998, 80, 4502.

[34] Kim, Y.-H., Sim, H.-S., Chang, K.-J. Electronic structure of collapsed C, BN, and BC3 nanotubes. Current Applied Physics. 2001, 1, 39-44.

[35] Kim, Y.-H., Chang, K.-J., Louie, S. Electronic structure of radially deformed BN and BC 3 nanotubes. Physical Review B. 2001, 63, 205408.

[36] Jalili, S., Akhavan, M., Schofield, J. Electronic and structural properties of bc3 nanotubes with defects. The Journal of Physical Chemistry C. 2012, 116, 13225-30.

[37] Nardelli, M.B., Yakobson, B.I., Bernholc, J. Brittle and ductile behavior in carbon nanotubes. Physical review letters. 1998, 81, 4656.

[38] Nardelli, M.B., Yakobson, B.I., Bernholc, J. Mechanism of strain release in carbon nanotubes. Physical review B. 1998, 57, R4277.

[39] Stone, A.J., Wales, D.J. Theoretical studies of icosahedral C60 and some related species. Chemical Physics Letters. 1986, 128, 501-3.

[40] Pan, B., Yang, W., Yang, J. Formation energies of topological defects in carbon nanotubes. Physical Review B. 2000, 62, 12652.

[41] Orellana, W., Fuentealba, P. Structural, electronic and magnetic properties of vacancies in single-walled carbon nanotubes. Surface science. 2006, 600, 4305-9.

[42] Rossato, J., Baierle, R., Orellana, W. Stability and electronic properties of vacancies and antisites in B C 2 N nanotubes. Physical Review B. 2007, 75, 235401.

[43] Berber, S., Oshiyama, A. Reconstruction of mono-vacancies in carbon nanotubes: atomic relaxation vs. spin polarization. Physica B: Condensed Matter. 2006, 376, 272-5.

[44] Li, Y., Zhou, Z., Golberg, D., Bando, Y., Schleyer, P.v.R., Chen, Z. Stone− wales defects in single-walled boron nitride nanotubes: formation energies, electronic structures, and reactivity. The Journal of Physical Chemistry C. 2008, 112, 1365-70.

[45] Piquini, P., Baierle, R.J., Schmidt, T., Fazzio, A. Formation energy of native defects in BN nanotubes: an ab initio study. Nanotechnology. 2005, 16, 827.

[46] Schmidt, M.W., Baldridge, K.K., Boatz, J.A., Elbert, S.T., Gordon, M.S., Jensen, J.H., et al. General atomic and molecular electronic structure system. Journal of Computational Chemistry. 1993, 14, 1347-63.

[47] Wong, M.W. Vibrational frequency prediction using density functional theory. Chemical Physics Letters. 1996, 256, 391-9.

[48] Schleyer, P.v.R., Maerker, C., Dransfeld, A., Jiao, H., van Eikema Hommes, N.J. Nucleus-independent chemical shifts: a simple and efficient aromaticity probe. Journal of the American Chemical Society. 1996, 118, 6317-8.

[49] Korotcenkov, G. Handbook of gas sensor materials. In: Conventional Approaches, Springer, 2013, Vol. 1.

[50] Richardson, O. Electron emission from metals as a function of temperature. Physical Review. 1924, 23, 153.

[51] Behmagham, F., Vessally, E., Massoumi, B., Hosseinian, A., Edjlali, L. A computational study on the SO2 adsorption by the pristine, Al, and Si doped BN nanosheets. Superlattices and Microstructures. 2016, 100, 350-7.

Figure captions

Fig. 1. Optimized structure of (a) BC_3 nanosheet, (b) AP drug.

Fig. 2. Optimized structure of different configuration of BC_3-AP.

Fig. 3. Optimized structure of (b) SV-BC_3 and (b) DV-BC_3.

Fig. 4. Optimized structure of (b) SV-BC_3@AP and (b) DV-BC_3@AP.

Fig. 5. Calculate total electron density maps of the energetically stable configuration for (a) BC_3-AP and DV-BC_3@AP.

Fig. 6. Variability of adsorption energy in DV-BC_3@AP in different solvents.

Table 1. The E_{ad} indicates the adsorption energy of AP drug on the BC_3 in kcal/mol. charge transfer and equilibrium distances for of BC_3-AP and SV-BC_3@AP and (b) DV-BC_3@AP.

Structure	E_{ad}	Q_T (e)	d (Å)
Complex I	-3.39	0.027	2.82
Complex II	-5.19	0.053	2.34
SV-BC_3@AP	-15.32	0.381	1.93
DV-BC_3@AP	-23.78	0.597	1.581

Fig.1

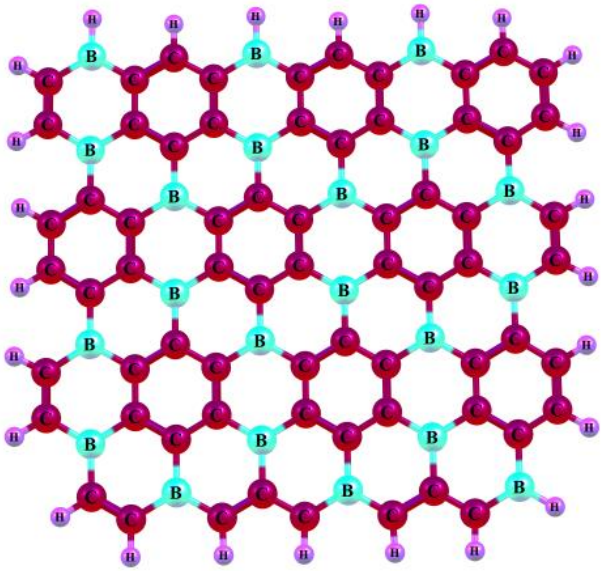

BC_3 nanosheet

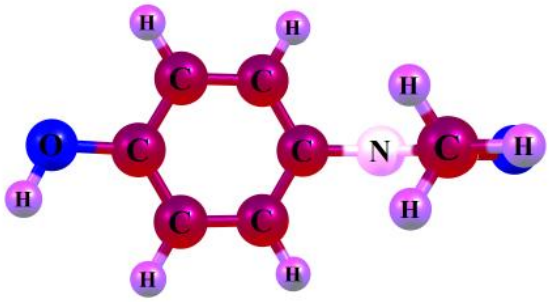

Acetaminophen drug

Fig. 2.

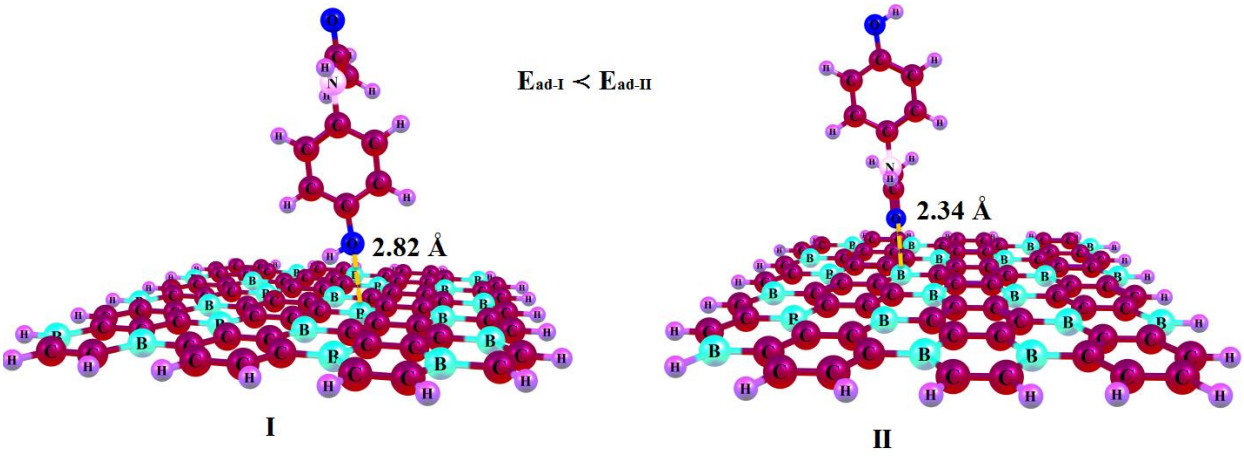

Fig.3

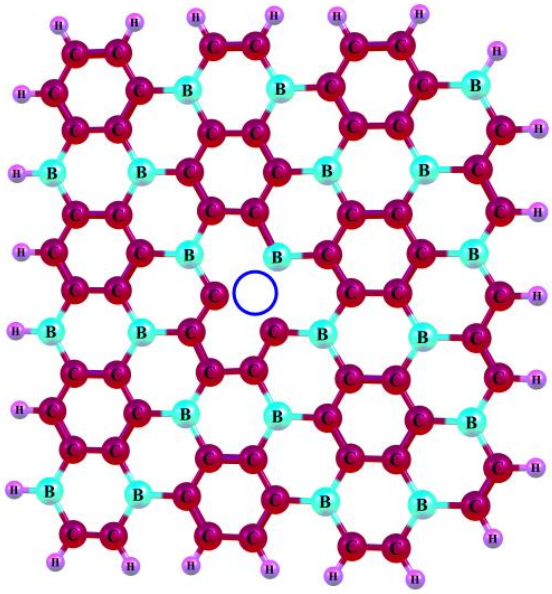

SV-BC_3

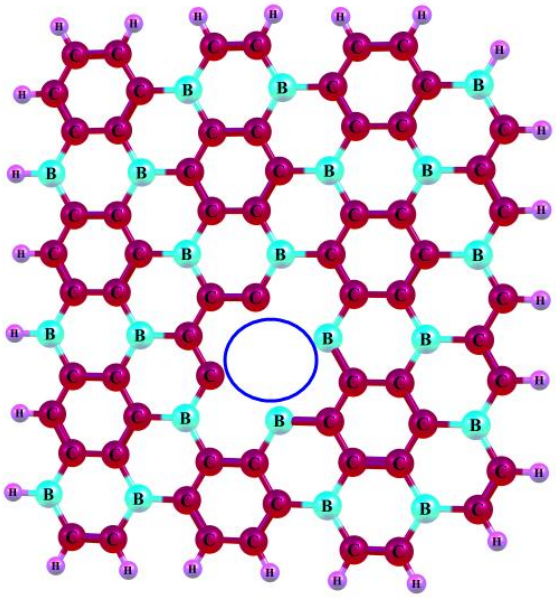

DV-BC_3

Fig.4

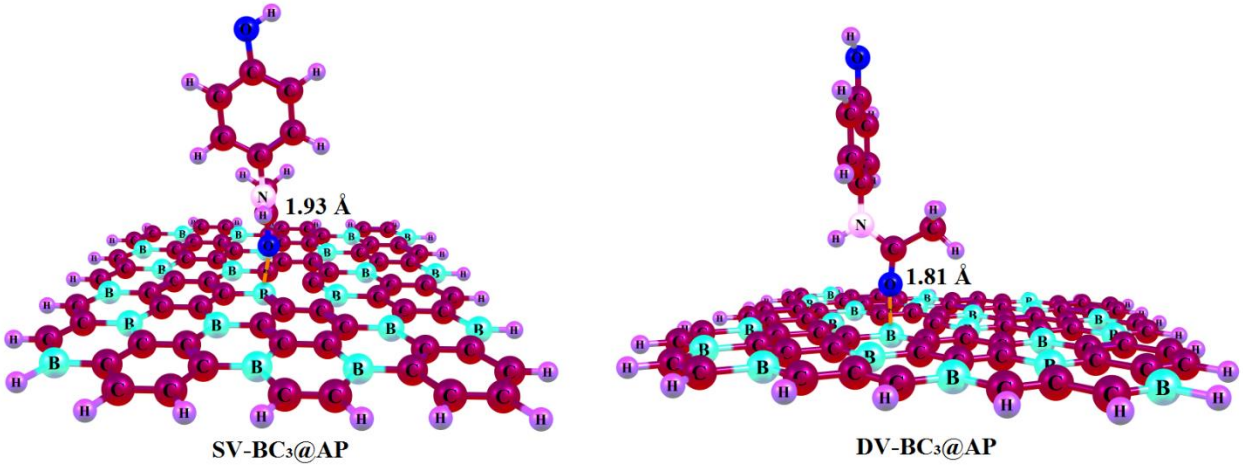

SV-BC_3@AP DV-BC_3@AP

Fig.5

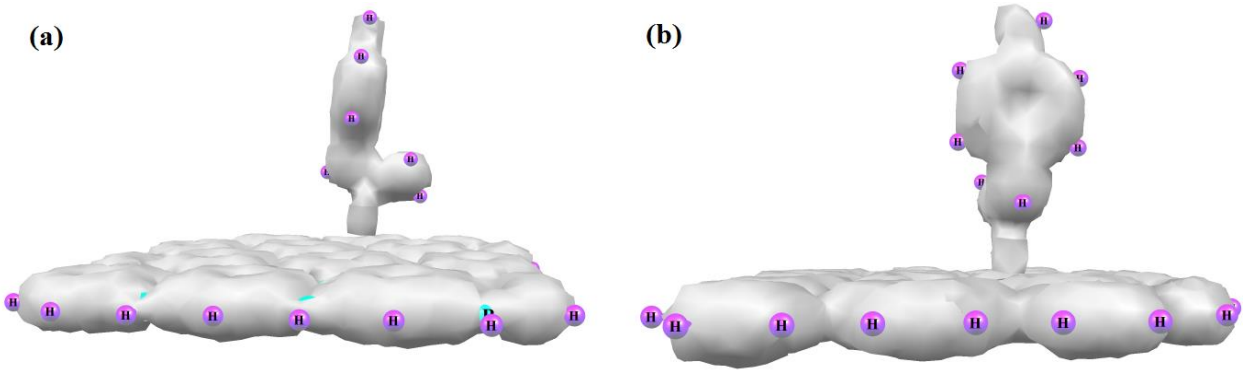

Fig.6

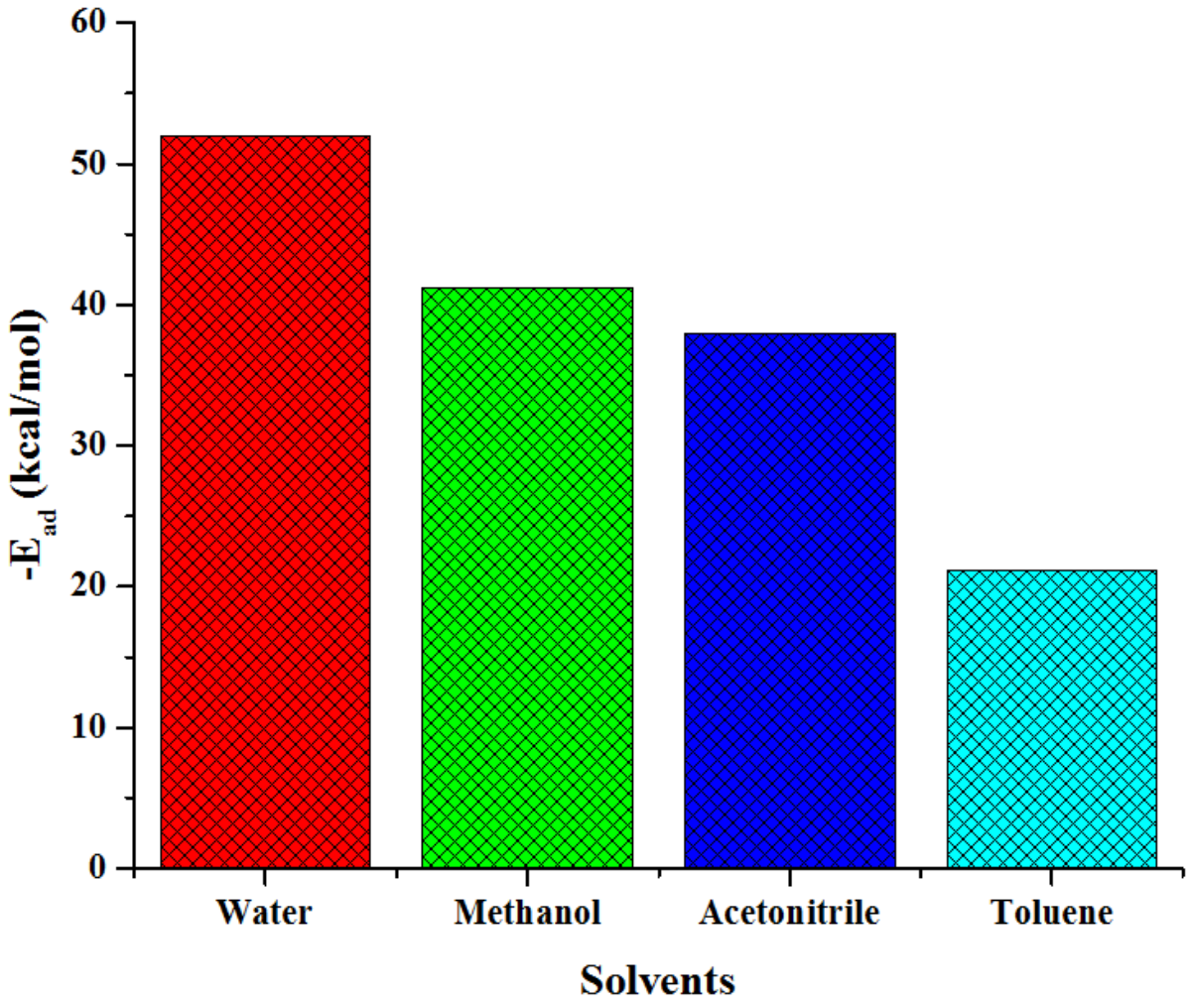
60
50
40
30
20
10
0
-E_ad (kcal/mol)
Water
Methanol
Acetonitrile
Toluene
Solvents

Figures

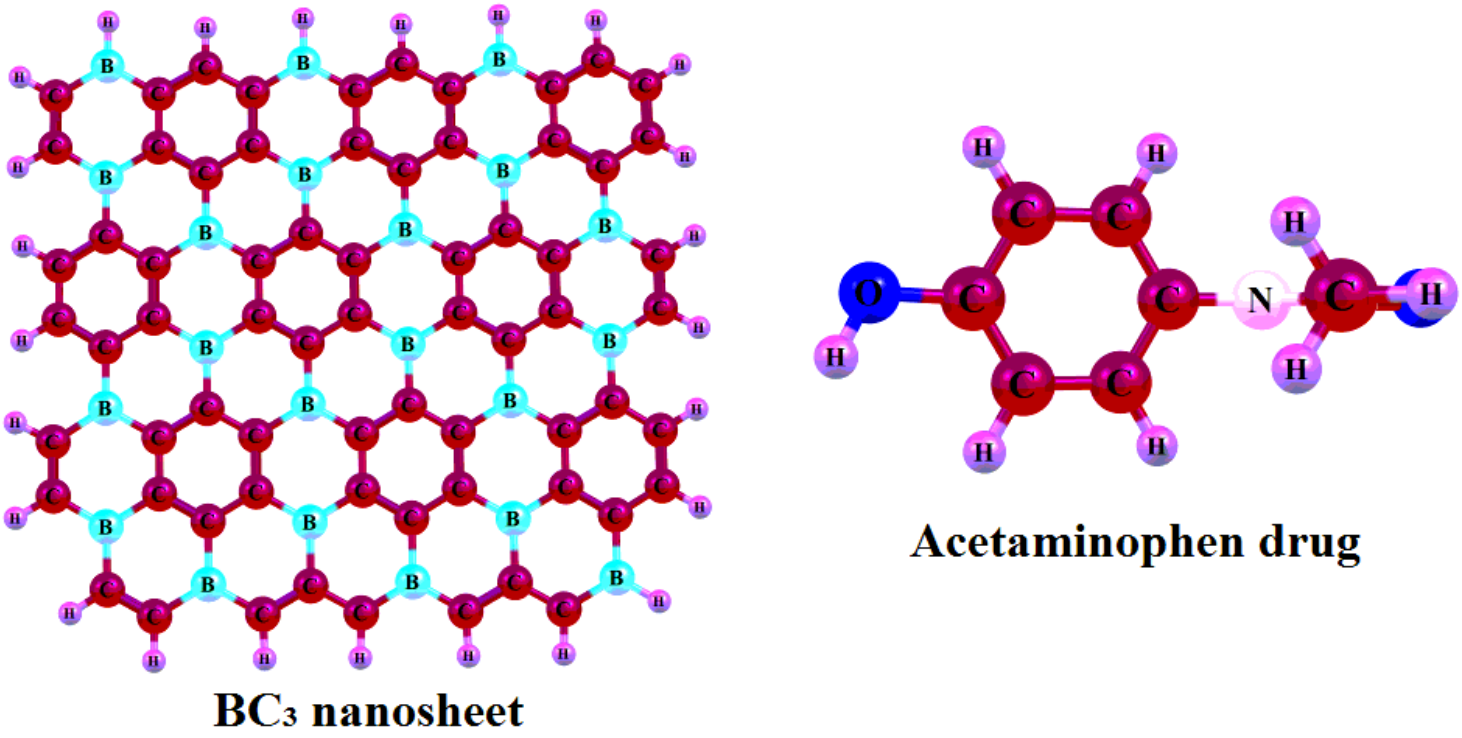

Figure 1

Optimized structure of (a) BC3 nanosheet, (b) AP drug.

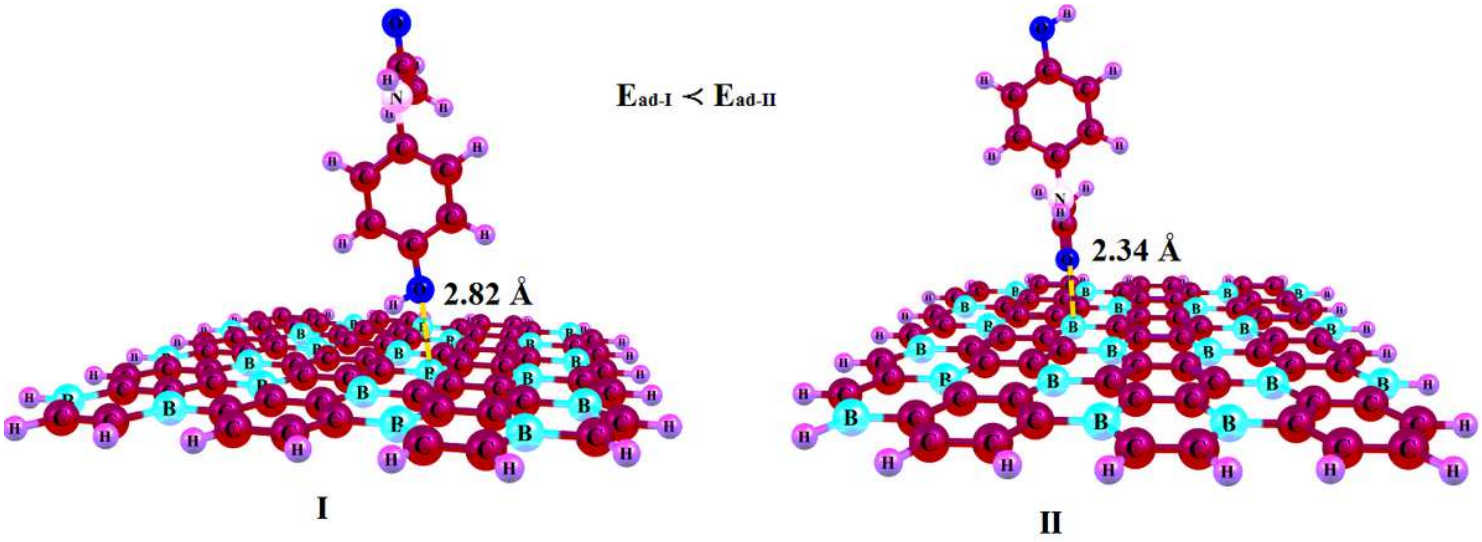

Figure 2

Optimized structure of different configuration of BC3-AP.

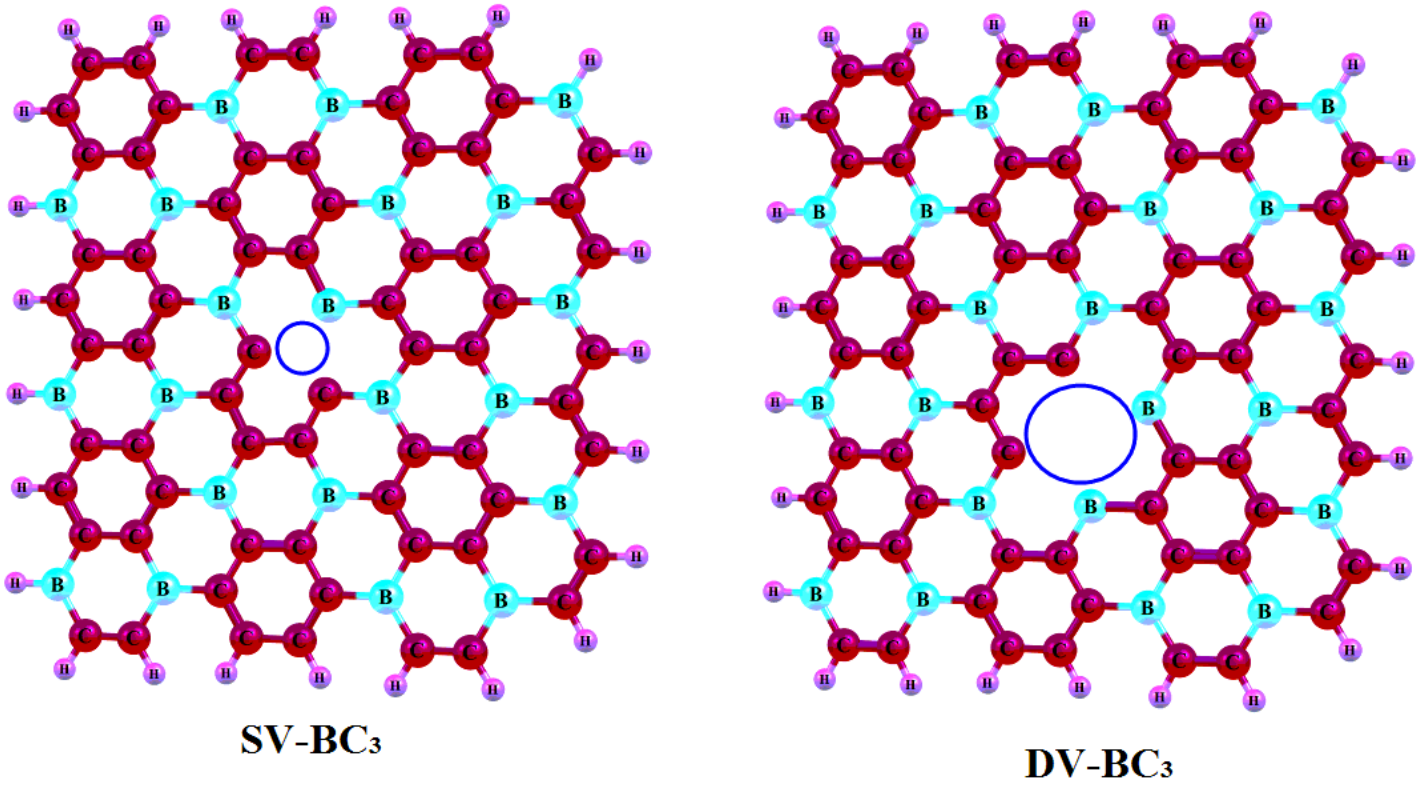

Figure 3

Optimized structure of (b) SV-BC3 and (b) DV-BC3.

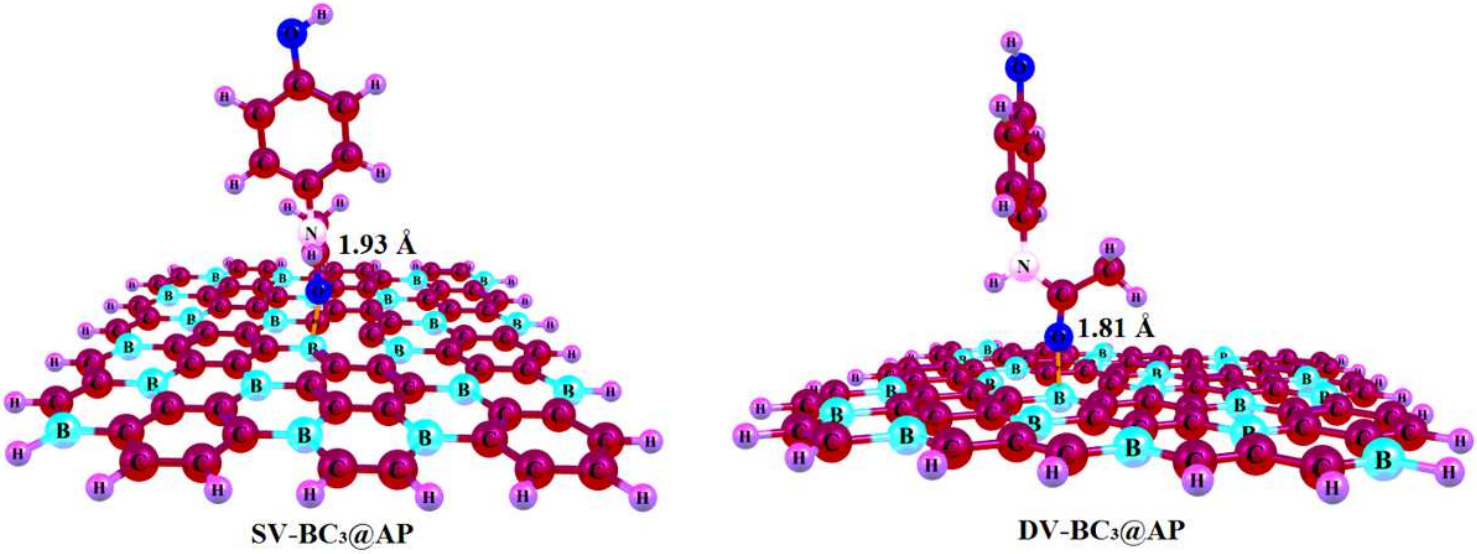

Figure 4

Optimized structure of (b) SV-BC3@AP and (b) DV-BC3@AP.

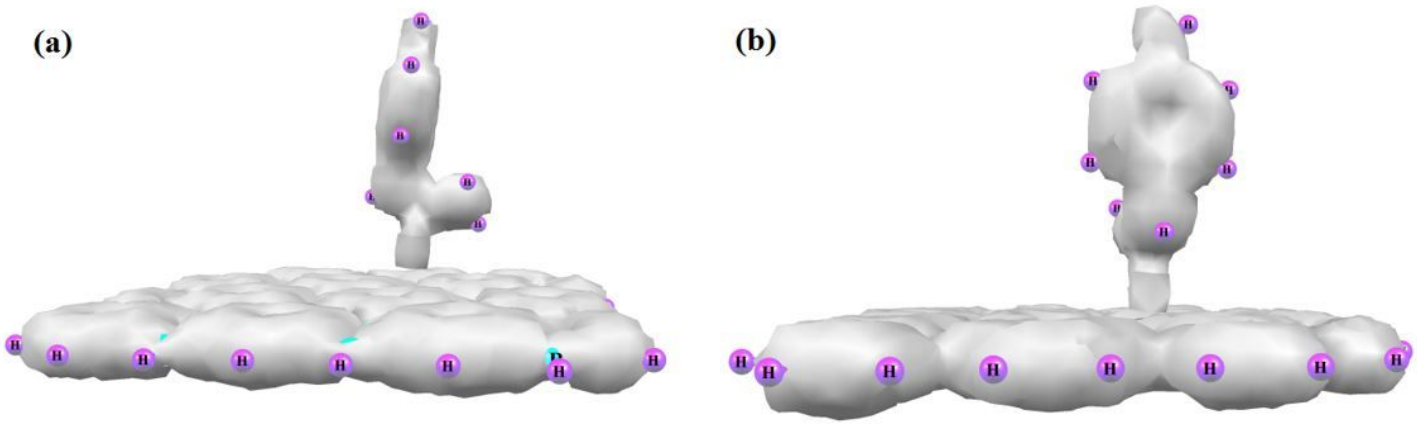

Figure 5

Calculate total electron density maps of the energetically stable configuration for (a) BC3-AP and DV-BC3@AP.

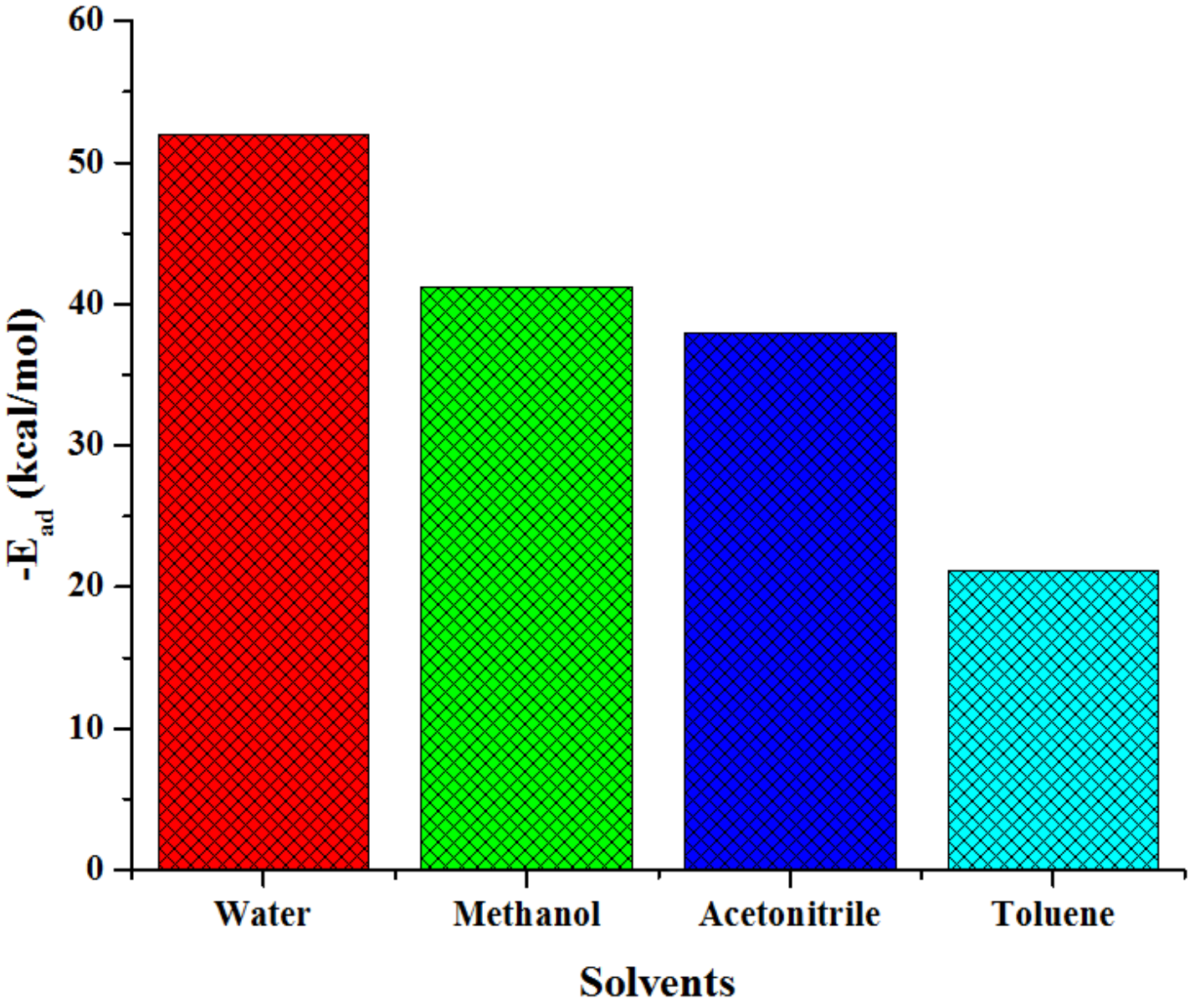

Figure 6

Variability of adsorption energy in DV-BC3@AP in different solvents.